

# Creating pseudo Kondo-resonances by field-induced diffusion of atomic hydrogen

Werner A. Hofer,<sup>1</sup> Gilberto Teobaldi,<sup>1</sup> and Nicolas Lorente<sup>2</sup>

<sup>1</sup>Surface Science Research Centre, the University of Liverpool, Liverpool L69 3BX, UK

<sup>2</sup>Institut de Ciència de Materials Barcelona, ICMAB-CSIC,

Campus UAB, Bellaterra, Barcelona 08913, Spain

(Dated: November 9, 2018)

In low temperature scanning tunneling microscopy (STM) experiments a cerium adatom on Ag(100) possesses two discrete states with significantly different apparent heights. These atomic switches also exhibit a Kondo-like feature in spectroscopy experiments. By extensive theoretical simulations we find that this behavior is due to diffusion of hydrogen from the surface onto the Ce adatom in the presence of the STM tip field. The cerium adatom possesses vibrational modes of very low energy (3–4meV) and very high efficiency ( $\geq 20\%$ ), which are due to the large changes of Ce-states in the presence of hydrogen. The atomic vibrations lead to a Kondo-like feature at very low bias voltages. We predict that the same low-frequency/high-efficiency modes can also be observed at lanthanum adatoms.

Scanning tunneling microscopy and spectroscopy (STM/STS) are at present the main tools to analyse the behavior of single atoms and molecules at conducting surfaces. Experiments at very low temperatures - typically around 4–5K - have contributed considerably to our understanding of single atom contacts [1], Kondo-resonances and their signature in the near-contact regime [2], spin-flip excitations of single atoms and atomic chains [3, 4], and vibrational excitations of single molecules [5]. Recently, the changes of electronic properties or atomic configurations due to field excitations were thoroughly investigated in STM experiments [6, 7, 8]. The salient feature in these experiments is the ability to modify the systems by varying the position and the field-intensity of the STM tip. However, the electronic properties of atoms can also be modified by the presence of hydrogen, as e.g. the measurements of Gupta *et al.* showed for nominally clean Cu(111) surfaces [9]. They obtained spectroscopic data with negative differential resistance, characteristic of vibrational excitations of a molecule [10]. Hydrogen itself, which is quite ubiquitous in a low-temperature ultra-high vacuum (UHV) environment, can only rarely be resolved in STM experiments [11]. Its effect on experimental scans has so far not been studied in great detail.

The aim of this Report is to demonstrate the ability of manipulating the position of atomic hydrogen at the nanometer scale by the field of an STM tip and to determine its effect in spectroscopy experiments at very low bias voltages. In this range, one typically detects a Kondo resonance for magnetic adatoms [2, 12], which is due to the interaction of a spin-state at a magnetic impurity with the conducting electrons of the underlying metal. Kondo resonances have a very characteristic signature, described by a Fano function [13, 14, 15]:

$$\frac{dI(V)}{dV} = A \frac{(\epsilon + q)^2}{1 + \epsilon^2} + B \quad (1)$$

with  $\epsilon = (eV - \epsilon_0)/\Gamma$ . In this equation,  $A$  is the amplitude coefficient,  $B$  is the background  $dI/dV$  signal,  $q$  is

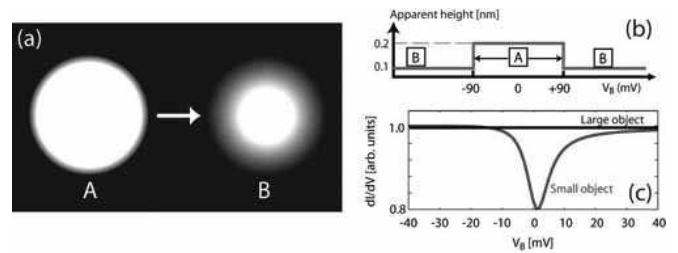


FIG. 1: Experimental results from [16]. (a) About 50% of the Ce adatoms are seemingly unstable and show two different (large A and small B) appearance (tunneling parameters in the experiments:  $V_T = -90$  mV,  $I_T = 100$  pA). (b) The unstable objects switch from a large protrusion of 200pm apparent height to a small protrusion of only 100pm apparent height if the bias voltage exceeds 90mV in either polarization. (c) Correspondingly, a Kondo-like resonance is observed at the unstable adatoms, while the stable adatoms reveal a completely flat  $dI/dV$  characteristic.

the Fano line shape parameter,  $\epsilon_0$  is the energy shift of the resonance from the Fermi level due to level repulsion between the  $d$ -level and the Kondo resonance, and  $\Gamma$  is the half width of the resonance.

In recent low-temperature experiments M. Ternes [16] found that adsorption of cerium atoms at Ag(100) surfaces leads to two different atomic species at the silver surface in low-temperature (4K) experiments. While most of the Ce adatoms remained stable and showed an apparent height of about 200pm in all STM scans, 5–50% of the adatoms were highly unstable depending on the applied bias voltage. For these objects it was found that a bias of  $\pm 90$ mV changes the apparent height from about 200pm to 100pm (see Fig 1(a) and (b)). In this case the structure remained stable as long as the STM tip remained at this location, even if the bias voltage was subsequently reduced to zero bias. The cause of this behavior could not be determined. In addition, STS ex-

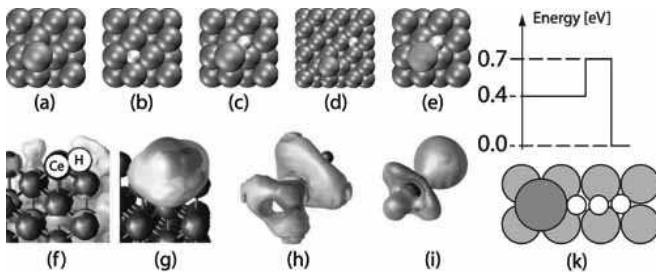


FIG. 2: Configurations in the DFT simulations (a-e), charge transfer (f-i) and diffusion barriers (k). (a) Ce adatom on Ag(100). (b) H atom adsorbed close to the surface plane of Ag atoms. (c) Ce with coadsorbed H. (d) Ce with H at a neighboring lattice site. (e) La with coadsorbed H. Charge depletion (f) and accumulation (g) of Ag(100) due to coadsorption of Ce and H. The adsorption creates a polar charge distribution at the surface. (h) and (i) Same for Ce and H in the adsorbed geometry but without Ag. Here, the Ce atom loses charge to hydrogen. (k) Relative energy of coadsorbed hydrogen, hydrogen at a neighboring bridge site, and hydrogen in a fourfold hollow site of Ag(100).

periments at very low bias at the bistable objects in its low-apparent-height state yielded a Fano function, which is characteristic for Kondo resonances of magnetic impurities. The  $q$ -value in the Fano fits was typically very low and in some cases even negative (see Fig. 1(c)). However, the change of conductance occurs at very low bias voltages, it is therefore well below the range where inelastic effects due to atomic vibrations are commonly observed.

To determine the cause of both effects, the change of apparent height of the Ce adatom under certain tunneling conditions, and the Fano-like behavior of the tunneling conductance at very low bias voltages, we performed extensive electronic structure simulations using density functional theory (DFT) and transport simulations for elastic and inelastic tunneling processes. It will be seen that both features have *one* common origin: the diffusion of hydrogen to the and coadsorption at the Ce adatom and the change of electronic properties as well as vibrational efficiencies due to the coadsorption. Finally, we tested the model for La adatoms, where a Kondo resonance is certainly impossible. In this case we predict a similar behavior as for Ce adatoms; a prediction which can be tested experimentally.

In Figure 2 (a) - (e) we show the groundstate configurations of the calculated systems [17]. All single adatoms adsorb at the fourfold hollow site. Coadsorbed hydrogen at Ce and La is close to a bridge position of the silver surface. The adsorption energy of hydrogen at Ag(100) is -2.84 eV (Configuration (b)), coadsorbed at Ce it is smaller and only -2.43 eV (Configuration (c)). From these results it can be concluded that the groundstate of the system is given by Ce and H, adsorbed at fourfold hollow sites. This result seems surprising at first

view, because Ce is routinely used in ultrahigh-vacuum chambers to remove hydrogen. One would thus expect that the coadsorption of Ce and H should be more favorable. To clarify this important point we also simulated  $H_2$ , CeH, and  $CeH_2$  in a vacuum, using the B3LYP functional. Here, we obtained a binding energy of -4.10 eV for  $H_2$ , in good agreement with experiments (-4.51 eV[18]), of -1.68 eV for CeH, and of -3.50 eV for  $CeH_2$ . For CeH, the corresponding value with standard functionals is -1.65 eV. From the difference in the binding energies of CeH and H/CeAg(100) it is clear that a significant proportion of the adsorption energy of coadsorbed hydrogen is due to bonding to the Ag(100) surface and not to Ce. This analysis leads to the unambiguous conclusion that coadsorbed hydrogen at Ce/Ag(100) is *not* the groundstate of the system by 0.41 eV. Calculating the total energy of H and CeAg(100) for hydrogen at an adjacent bridge site we find an energy barrier of +0.29 eV. The relative energies for hydrogen diffusion from its groundstate at the Ag(100) surface to Ce/Ag(100) are shown in Fig. 2(k). Given the position of coadsorbed hydrogen and the symmetry of the Ag(100) surface it is clear that four equivalent pathways exist for the diffusion of hydrogen from its groundstate position at the Ag(100) surface to Ce. However, it is not yet clear, under which conditions hydrogen will coadsorb at Ce at all. There have been a number of experiments, where diffusion of atomic hydrogen due to the field of the STM tip has been observed[11, 19]. A straightforward calculation of total energies under an applied dipole field could in principle elucidate the change of adsorption energy due to an applied bias. However, in case of CeH/Ag(100) DFT simulations did not arrive at a converged solution, presumably due to the large size and complexity of the system. To understand the effect of an external field on CeH/Ag(100) we simulated the charge transfer by subtracting the charge density of the system components from the charge density of the coupled system. We find that CeH leads to the occurrence of a dipole moment in vertical direction since charge is removed from the Ag(100) surface and accumulated at the position of CeH (Fig. 2(f) and (g), the value of the contour is +0.001e/Å<sup>3</sup>, and -0.006e/Å<sup>3</sup>, respectively). The change of total energy due to a tip field  $\mathbf{E}_{tip}$  is given by [20]:

$$\Delta E = -\mathbf{P}_0 \mathbf{E}_{tip} - \alpha \chi_e |\mathbf{E}_{tip}|^2 \quad (2)$$

Here,  $\mathbf{P}_0$  is the residual dipole moment of CeH,  $\alpha$  is a constant, and  $\chi_e$  is the electric susceptibility. Due to the much higher number of valence electrons in Ce it can be expected that  $\chi_e$  is much larger for CeH/Ag(100) than for H/Ag(100). From the charge difference contours we may conclude that the total charge accumulated in the surface dipole is less than 0.05 electrons; the residual dipole, and consequently the asymmetric changes of total energy with an applied tip field will be rather small. The dominating term in the energy change should thus be due

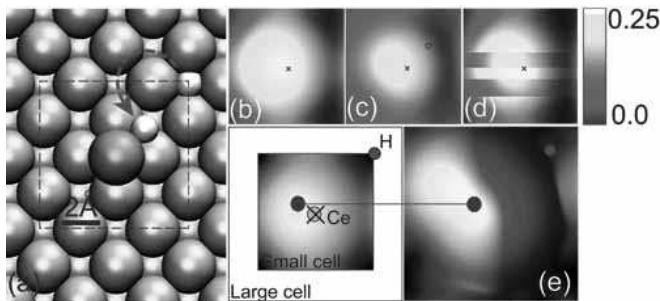


FIG. 3: STM simulations of the switching feature observed on Ce adatoms. (a) at a finite voltage increase the hydrogen atom diffuses across a barrier and attaches to the Ce adatom (see arrow). (b) Constant density contour for Ce adatom, and (c) for Ce adatom with coadsorbed hydrogen. (d) The contour changes its vertical distance by more than  $1\text{\AA}$ . (e) Shift of the contour maximum due to hydrogen at a neighbouring lattice site. The maximum shifts by about  $1\text{\AA}$  compared to the contour at a clean Ag(100) surface (yellow circle) if hydrogen is adsorbed at a neighboring lattice site (hydrogen: grey circle, new contour maximum: red circle).

to induced dipoles (the second term in Eq. 2), which is symmetric with the applied field intensity. In this case we expect that a certain threshold intensity in both polarizations will lower the total energy of CeH/Ag(100) enough, so that it becomes more favorable than the groundstate Ce+H/Ag(100). In this case hydrogen will diffuse across the surface and coadsorb on Ce. Given that the field for an atomically sharp tip is confined to a radius of less than  $1\text{nm}$  [21], diffusion will occur only in the immediate vicinity of the STM tip and thus the position of the Ce adatom. We may thus conclude that the higher susceptibility of Ce compared to H leads to diffusion of hydrogen along the Ag(100) surface. However, once CeH is formed, the diffusion barrier of  $0.29\text{eV}$  will retain H at Ce, even if the bias voltage is decreased. This conclusion is also in line with experimental data. From the diffusion barrier of  $0.29\text{eV}$  we may finally conclude, that a voltage pulse of  $0.3\text{V}$  should be sufficient for H to overcome the barrier and diffuse along the surface. Given the high mobility of H even at low temperature, we can thus predict that the observed object will change again at higher positive bias voltages.

To determine the changes of the contours upon coadsorption of hydrogen we performed STM simulations as described in the methods section. The adatom appears as a bright protrusion with an apparent height of about  $2.5\text{\AA}$  (Fig. 3(b)), and a diameter of about  $7\text{\AA}$ , in accordance with experimental images of the (i) large stable, and (ii) large unstable atom. Subsequently, we simulated coadsorbed hydrogen at the Ce adatom and determined the ensuing constant density contours. Using the contour value for the bare adatoms, we find that the density contours on top of Ce are now  $1.2\text{\AA}$  closer to the surface, in

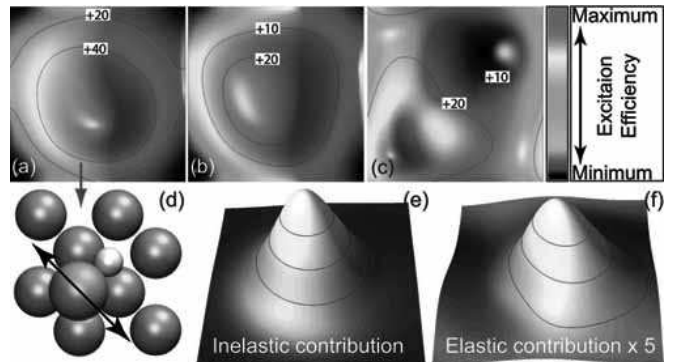


FIG. 4: Efficiency of two low-energy vibrational excitations for Ce adatoms and coadsorbed hydrogen (a-b) and La with coadsorbed hydrogen (c). The colormap scale bar indicates the spatially resolved efficiency. The efficiency is positive in all cases, the mode with the highest efficiency, at  $3.7\text{ meV}$  (frame (a)), is due to Ce-motion constrained by coadsorbed of hydrogen (see frame (d)). (e-f) High-efficiency mode of Ce/H. The inelastic efficiency is centered at the position of the Ce adatom (e) and substantially larger than the elastic component (f).

line with experimental findings (Fig. 3(c) and (d))[16]. The reason for the lower contour is the decrease of density at the position of the Ce adatom, as can be seen in the charge difference contours of CeH in Fig. 2(h) and (i). From the simulations we may thus conclude that the switching behavior of Ce adatoms is due to reversible diffusion and coadsorption of hydrogen. We also simulated the shift of a contour maximum, which should in principle be detectable in STM scans, from an isolated Ce adatom to a system where H is adsorbed at a neighboring hollow site (Fig. 2(d)). Here, we find that the contour is displaced by about  $1\text{\AA}$ . Given the symmetry of the system, we expect four equivalent shifts to occur in the experiments. An analysis of the  $f$ -states of Ce reveals that due to their position at the Fermi level the Kondo temperature should be well below the temperature in the experiments ( $4\text{K}$ )[2]: Kondo-resonances in this system are therefore not measurable. This initial finding suggested to search for a different origin. The only potential origin in this case are atomic vibrations. In order to model low-energy vibrational excitations, we solved the dynamical matrix for ionic motion of the Ce adatom, the hydrogen adatom, and the silver surface layer keeping the other ionic positions fixed. We find low-energy vibrational modes between  $3\text{--}4\text{ meV}$  for both systems, Ce/Ag(100) and CeH/Ag(100). The reason for the very low excitation energy is the very high mass of cerium. The coupling to a vibrational mode of molecules depends on a superposition of elastic and inelastic contributions to the tunneling current, which yield a reduction and an increase in current, respectively [22, 23]. The total efficiency of a vibrational mode thus depends significantly on the su-

perposition of these two contributions [24]. Due to this effect, the total efficiencies for the Ce/Ag(100) system in the low energy range are close to zero for all calculated vibrational modes. However, this changes drastically for systems with coadsorbed hydrogen. In Fig. 4 (a-b) we show the total efficiencies of two low-energy vibrational modes as a function of position for CeH/Ag(100). At the position of the Ce atom the efficiency in this case is higher than 20% (Fig. 4 (b)), or even 40% (Fig. 4 (a)). Given that the efficiency determined from constant density contours is generally overestimated by a factor of about two, the results for vibrational efficiencies under the condition of hydrogen coadsorption agree very well with the experiments (about 20% in [16]). At  $T=0$  K the signature of a vibration in the  $dI/dV$  spectrum is a step in the conductance at 3–4 mV in both polarizations; due to thermal broadening it will be measured as an asymmetric feature: onset from 0 mV, reaching its maximum of 20% increase at 6–8 mV, and nearly flat with a gradual decrease above 8 mV [9] (see Fig. 1(c)); a signature which is very similar to a Kondo-resonance (dip at the Fermi level). The coadsorption of hydrogen on La/Ag(100) leads to a vibrational efficiency in the same range of 20–30% at 3.5 meV (Fig. 4 (c)). Pending the verification by STM experiments, we may conclude on the basis of simulations that (i) the Kondo-like resonance is actually due to inelastic excitations, and (ii) that these excitations will also be observed for other adatoms in the presence of coadsorbed hydrogen. While for bare Ce, the elastic components are nearly equal or even larger than the inelastic ones, the coadsorption of hydrogen leads to a decrease of the elastic efficiency, and, consequently to an increase of the overall efficiency. An analysis of the high-efficiency phonon mode at 3.7 meV reveals that it is due to a constrained vibration of cerium. The mode is shown in Fig. 4 (d), the inelastic and elastic efficiencies in Fig. 4 (e), and (f), respectively. In the higher energy range above 5meV we found several vibrational modes, both for Ce/Ag(100) and CeH/Ag(100). However, the amplitude of the coupling for vibrational excitations is inversely proportional to the excitation energy [25]. While a low frequency excitation with an efficiency of about 20% can therefore easily be detected at 3–4 meV, the ensuing increase in the  $dI/dV$  spectrum will be less than 10% for 8 meV, and below 5% for 16 meV, which corresponds roughly to the detection limit in the experiments. Considering, in addition, that the superposition of elastic and inelastic contributions in most cases makes these vibrations invisible by scanning tunneling spectroscopy, it is reasonable to assume that the higher energy modes will not leave a measurable signature in the experimental scans.

To summarize, we found that dynamic processes of hydrogen adsorption and diffusion, manipulated by the field of the STM tip, play a pivotal role in low temperature experiments. These processes lead to a bistable switching behavior of single adatoms. Here, vibrational modes

of unusually low energies and unusually high efficiencies have the same appearance as a typical Kondo-resonance. What seems most interesting in this study is the possibility of engineering subtle physical properties reversibly at the single-atom level by field-induced diffusion processes.

**Acknowledgements:** Helpful discussions with Wolf-Dieter Schneider (EPFL Lausanne) and Markus Ternes (IBM Almaden) are gratefully acknowledged. WAH is supported by the Royal Society, GT is funded by EPSRC grant EP/C541898/1.

- 
- [1] L. Limot, J. Kroger, R. Berndt, A. Garcia-Lekue, and W. A. Hofer, Phys. Rev. Lett. **94**, 126102 (2005).
  - [2] N. Neel, J. Kroger, L. Limot, K. Palotas, W. A. Hofer, and R. Berndt, Phys. Rev. Lett. **98**, 016801 (2007).
  - [3] A. J. Heinrich, J. A. Gupta, C. P. Lutz, and D. M. Eigler, Science **306**, 466 (2004).
  - [4] C. F. Hirjibehedin, C. P. Lutz, and A. J. Heinrich, Science **312**, 1021 (2006).
  - [5] B. C. Stipe, M. A. Rezaei, and W. Ho, Science **280**, 1732 (1998).
  - [6] M. Lapstapis, M. Martin, D. Riedel, L. Hellner, G. Comtet, and G. Dujardin, Science **308**, 1000 (2006).
  - [7] J. A. Stroscio, F. Tavazza, J. N. Crain, R. J. Celotta, and A. M. Chaka, Science **313**, 948 (2006).
  - [8] K. R. Harikumar, J. C. Polanyi, P. A. Sloan, S. Ayissi, and W. A. Hofer, J. Am. Chem. Soc. **128**, 16791 (2006).
  - [9] J. A. Gupta, C. P. Lutz, A. J. Heinrich, and D. M. Eigler, Phys. Rev. B **71**, 115416 (2005).
  - [10] J. Gaudio, L. J. Lauhon, and W. Ho, Phys. Rev. Lett. **85**, 1918 (2000).
  - [11] C. Klein, A. Eichler, E. L. D. Hebenstreit, G. Pauer, R. Koller, A. Winkler, M. Schmid, and P. Varga, Phys. Rev. Lett. **90**, 176101 (2003).
  - [12] U. Fano, Phys. Rev. **124**, 1866 (1961).
  - [13] V. Madhavan, W. Chen, T. Jamneala, M. F. Crommie, , and N. S. Wingreen, Phys. Rev. B **64**, 165412 (2001).
  - [14] P. S. Cornaglia and C. A. Balseiro, Phys. Rev. B **67**, 205420 (2003).
  - [15] J. Merino and O. Gunnarson, Phys. Rev. B **69**, 115404 (2004).
  - [16] M. Ternes, *Scanning Tunneling Spectroscopy at the Single Atomic Scale*, Ph.D. thesis, École Polytechnique Fédérale de Lausanne, These No. 3465, web: library.epfl.ch/en/theses/?nr=3465 (2006) pp. 59–67.
  - [17] **Methods:** The Ag(100) surface was mimicked by a seven-layer  $3\times 3$  silver unit-cell, with a vacuum range of at least  $15\text{\AA}$ , using VASP [26] in its projector-augmented wave implementation [27], with a sampling of the Brillouin zone with  $4\times 4$  special  $k$ -points. Exchange-correlation energies were described by the PBE functional [28]. The energy cutoff in the simulations was 500 eV. The Ce, La and H adatom was fully relaxed together with the first layer of the silver surface. STM simulations were performed with bSKAN [29, 30], first with a clean metal tip for a few points of the unit cell. Given the large energy cutoff, we simulated the local density contours at the appropriate distance for the tunneling parameters of the experiments (typically -90 mV and

- 100 pA). The maximum distance above the isolated Ce adatom is  $5.3\text{\AA}$ . The phonon efficiencies were calculated using the theoretical method developed by Lorente and Persson [24, 31]. The ratio between the sum of elastic and inelastic contributions divided by the normal contribution, i.e. the groundstate density, at this bias voltage in this case gives the efficiency  $\eta$  of a vibrational mode [24].
- [18] D. R. Lide (ed.), *Handbook of Chemistry and Physics* (2007).
- [19] J. A. Stroscio and D. M. Eigler, *Science* **254**, 1319 (1991).
- [20] J. D. Jackson, *Classical Electrodynamics* (1998).
- [21] K. Stokbro, *Surf. Sci.* **429**, 327 (1999).
- [22] T. Mii, S.G.Tikhodeev, and H. Ueba, *Phys. Rev. B.* **68**, 205406 (2003).
- [23] N. Agrait, C. Untiedt, G. Rubio-Bollinger, and S. Vieira, *Phys. Rev. Lett.* **88**, 216803 (2002).
- [24] N. Lorente, *Appl. Phys. A* **78**, 799 (2004).
- [25] A. Eiguren, B. Hellsing, E. Chulkov, and P. Echenique, *Phys. Rev. B* **67**, 235432 (2003).
- [26] G. Kresse and J. Hafner, *Phys. Rev. B* **47**, 558 (1993).
- [27] G. Kresse and D. Joubert, *Phys. Rev. B* **59**, 1758 (1999).
- [28] J. P. Perdew, M. Ernzerhof, and K. Burke, *J. Chem. Phys.* **105**, 9982 (1996).
- [29] K. Palotas and W. A. Hofer, *J. Phys.: Cond. Mat.* **17**, 2705 (2005).
- [30] W. A. Hofer, *Prog. Surf. Sci.* **71**, 147 (2003).
- [31] N. Lorente, M. Persson, L. J. Lauhon, and W. Ho, *Phys. Rev. Lett.* **86**, 2593 (2001).